A dynamic model of nutrient uptake by root hairs

D. Leitner[1,6], S. Klepsch[1,7], M. Ptashnyk[2,6], A. Marchant[3], G. J. D. Kirk[4], A. Schnepf[1] and T. Roose[5,6]

[1]Department of Forest and Soil Sciences, Institute of Soil Research, BOKU-University of Natural Resources and Applied Life Sciences, Peter Jordan-Straße 82, 1190 Vienna, Austria; [2]Institute of Applied Mathematics, University of Heidelberg, IWR, Im Neuenheimer Feld 294, 69120 Heidelberg, Germany; [3]School of Biological Sciences, University of Southampton, Boldrewood Campus, Southampton SO16 7PX, UK; [4]National Soil Resources Institute, Cranfield University, Cranfield MK43 0AL, UK; [5]School of Mathematics, University of Southampton, University Road, Southampton SO17 1BJ, UK; [6]Mathematical Institute, Oxford Centre for Industrial and Applied Mathematics and Centre for Mathematical Biology, University of Oxford, 24 - 29 St. Giles, Oxford OX1 3LB, UK; [7]Health & Environment Department, AIT Austrian Institute of Technology, A-2444 Seibersdorf, Austria

Summary

- Root hairs are known to be important in the uptake of sparingly soluble nutrients by plants, but quantitative understanding of their role in this is weak. This limits, for example, the breeding of more nutrient-efficient crop genotypes.
- We developed a mathematical model of nutrient transport and uptake in the root hair zone of single roots growing in soil or solution culture. Accounting for root hair geometry explicitly, we derived effective equations for the cumulative effect of root hair surfaces on uptake using the method of homogenization.
- Analysis of the model shows that, depending on the morphological and physiological properties of the root hairs, one of three different effective models applies. They describe situations where: (1) a concentration gradient dynamically develops within the root hair zone; (2) the effect of root hair uptake is negligibly small; or (3) phosphate in the root hair zone is taken up instantaneously. Furthermore, we show that the influence of root hairs on rates of phosphate uptake is one order of magnitude greater in soil than solution culture.
- The model provides a basis for quantifying the importance of root hair morphological and physiological properties in overall uptake, in order to design and interpret experiments in different circumstances.

Introduction

Root hairs are lateral extensions of epidermal cells, and these root hairs increase the effective surface area of the root system available for water and nutrient uptake. They are particularly important for nutrients that are sparingly soluble in the soil, such as phosphate (Marschner, 1995). The widths of phosphorus-depletion zones around nonmycorrhizal roots are closely related to root hair length, and plants grown under phosphate-limiting conditions form longer root hairs (Bates & Lynch, 1996; Zhang *et al.*, 2003). Conversely, mutant plants with impaired root hair growth–such as root-hair-defective *Arabidopsis* mutants *rhd2* and *rhd6*, which are involved in hair initiation and elongation respectively–have a reduced capacity for phosphate uptake under phosphate-limiting conditions (Bates & Lynch, 2000a). A better understanding of how root hairs

mediate phosphate uptake will enhance the development of more phosphate-efficient crops. This can help to minimize fertilizer use and pollution risk (Narang *et al.*, 2000; Wissuwa, 2003). Given the complexity of root hair–soil interactions, and the difficulty of measuring these interactions experimentally, development of mathematical models is necessary. Mathematical models will enable comparisons to be made between different root hair properties, such as their geometry and rates of nutrient uptake.

Previous approaches to modelling root hair in nutrient-uptake models fall in three categories. First, the effective root radius is extended by the length of the hairs, and any concentration gradients along the hair length are not allowed for (Passioura, 1963). Second, the continuity equation for nutrient transport to the root surface is modified with a separate sink term describing nutrient influx into the hairs (Bhat *et al.*, 1976). Third, the nutrient transport

equation is solved in a three-dimensional model that takes into account the geometry of root hairs explicitly (Geelhoed et al., 1997).

Modelling such multiscale problems in three dimensions is computationally challenging and generally beyond the scope of standard numerical methods (such as Comsol Multiphysics, PHREEQC, Orchestra, MIN3P, etc.) used in rhizosphere research. While three-dimensional numerical simulations could be utilized to address single root scale phenomena, they are usually very costly and the translation of such results from single root scale to root system scale and field scale is seriously challenging. For such multiscale problems, such as root hair nutrient uptake, the homogenization method (Pavliotis & Stuart, 2008) provides a possible solution. With this method, spatial heterogeneities at different scales can be transformed into a tractable homogeneous description. Equations that are valid on a macroscale are derived by transparently incorporating the relevant information about the microscale geometry and model properties.

The method of homogenization is particularly suitable for domains with a periodic microstructure. The microstructure of root hairs is illustrated in Fig. 1(a). On the left of Fig. 1(a) the different properties of root hairs and the surrounding soil solution are illustrated by periodic changes of dark and light regions. The microscopic length scale is given by the inter-root hair distance, l. If the ratio between the single root hair scale, l, and root length scale, L, is small (i.e. $\epsilon = l/L << 1$), it is possible to derive an effective macroscopic model describing the root hair zone function. In the graph on the left of Fig. 1(a) the heterogeneities can be distinguished. However, viewed from a distance, as in the graph shown on the right of the figure, the heterogeneities average out. This is, in essence, what the homogenization technique does: it describes how the root hair functions blend into the model viewed on the coarser root length scale. The space variable, x, reveals the properties of the system on the scale of the whole root hair zone. Scaling x with ϵ^{-1} defines a new space variable, $y = x\epsilon^{-1}$, which reflects the microscopic properties on the scale of the single root hair. One of the fundamental assumptions of homogenization is that the two variables x and y can be treated as independent of each other when ϵ becomes small (Pavliotis & Stuart, 2008). A well-known example is the macroscopic Darcy law derived from the Stokes equations (Hornung, 1997), whereby the role of exact particle shape on hydraulic permeability can be explained.

In this work, we use the method of homogenization to develop an effective model of nutrient transport in the root hair zone of a single root that contains the relevant information about the root hair geometry implicitly. We consider a root with root hairs in a homogeneous medium. In the case of soil, this is a major simplification because the root hair size can be comparable to the soil particle size. We will
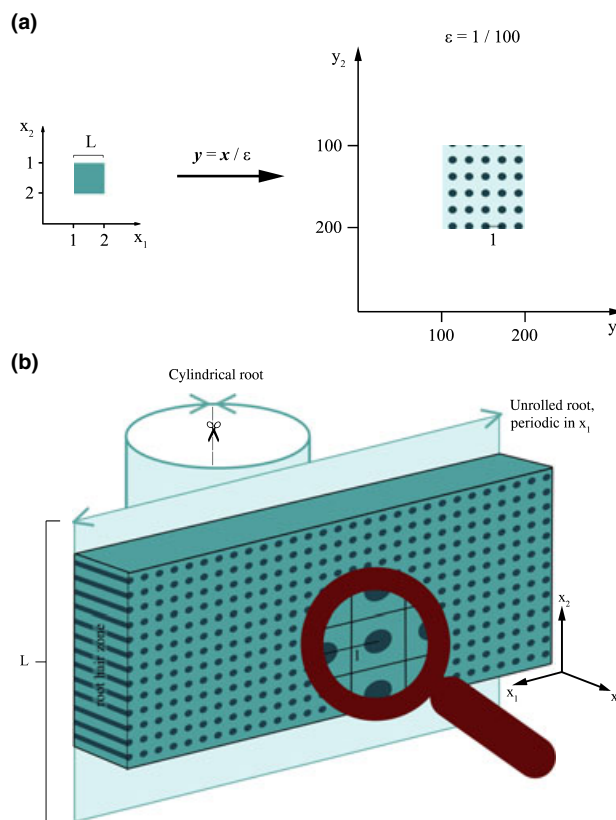

Fig. 1 The geometry of the model. (a) The upper figure illustrates homogenization across scales. The graph shown on the right is in coarse $x = (x_1, x_2, x_3)$ coordinates and shows the macrostructure of the system; the macroscopic length scale, L, is the root length. The graph shown on the left is in finer $y = (y_1, y_2, y_3)$ coordinates and reveals the microstructure; the microscopic length scale, l, is the inter hair distance. The scaling parameter, $\epsilon = l/L$, describes the reduction of the level of detail from microstructure to macrostructure. (b) The lower part of the figure shows a cylindrical root with axial length L. The root surface is rolled out and can therefore naturally be described in Cartesian coordinates. The root hairs are perpendicular to the root surface; in this way the root hair zone is described by a rectangular domain.

address this issue in a follow-up paper, but for now we assume that the soil around each root hair is homogeneous (Bhat et al., 1976; Geelhoed et al., 1997).

We analyse the development of nutrient-depletion zones around a root with root hairs for different root morphologies and uptake properties and thereby obtain three different effective models. The notation used is given in Table 1.

Materials and Methods

Dimensional model explicitly considering root hair geometry

We consider a single root with a root hair zone in a homogeneous medium. The medium may be either soil or nutri-

Table 1 The parameters and variables used in the dimensional model

Symbol	Description
a_h, a_r	Root hair and root radius (cm)
b	Soil buffer power (−)
c	Nutrient concentration in the solution (μmol ml^{-1})
c_a	Effective nutrient concentration in the root hair zone V_a (μmol ml^{-1})
c_b	Nutrient concentration in the domain outside the root hair zone V_b (μmol ml^{-1})
c_0	Initial solution concentration at time $t = 0$ (μmol ml^{-1})
d	Factor that distinguishes between solution culture and soil systems. In the solution culture $d = 1$; in soil $d = 1/(\theta + b)$ (−)
D_l	Molecular diffusion coefficient of nutrients in solution (cm^2 s^{-1})
D	Diffusion coefficient; $D = D_l$ in solution culture, $D = D_l \theta f/(\theta + b)$ in soil (cm^2 s^{-1})
$\bar{D}$	Effective diffusion coefficient taking the impedance caused by root hairs into account (cm^2 s^{-1})
E_h, E_r	Efflux from root hairs and root (μmol cm^{-2} s^{-1})
f	Impedance factor of soil (−)
f_a	Effective root hair uptake (μmol cm^{-2} s^{-1})
f_h, f_r	Net influx into the root hair and root (μmol cm^{-2} s^{-1})
F_h, F_r	Maximal nutrient influx into root hairs and root (μmol cm^{-2} s^{-1})
K_h, K_r	Michaelis–Menten constants for root hairs and root (μmol ml^{-1})
l	Distance between two root hairs (cm)
L	Root length (cm)
L_h	Root hair length (cm)
n	Outer normal vector
N	Number of root hairs per cm root length (cm^{-1})
t	Time (s)
V_a	Root hair zone (cm^3)
V_b	Domain outside the root hair zone (cm^3)
α	The parameter $\alpha = \ln\left(\frac{l}{DK_h}F_h\right)/\ln\left(\frac{l}{L}\right)$ determines which effective model applies (−)
x	The vector $\mathbf{x} = (x_1, x_2, x_3)$ is the macroscopic space variable.
y	The vector $\mathbf{y} = (y_1, y_2, y_3)$ is the microscopic space variable.
θ	Volumetric water content excluding soil particles (−)
θ_h	Volumetric content of medium excluding root hairs, $\theta_h = 1 - \theta_{hair}$ (−)
θ_{hair}	Volume fraction of root hairs (−)

ent solution. In both cases nutrients move to absorbing roots by diffusion and convection. However, in soil there are the additional complications of the tortuosity of the soil pore network, and sorption of the diffusing nutrients on soil surfaces. Following Tinker & Nye (2000), we treat the soil as quasi-homogeneous at the scale of interest and average across micro-scale heterogeneities. In practice the assumption of quasi homogeneity is imperfect. However, a full treatment of micro-scale heterogeneity would unduly complicate the model. We define a composite soil diffusion coefficient that contains an impedance factor for tortuosity and a buffer power for sorption.

Furthermore, we consider Cartesian geometry rather than the more computationally complex cylindrical geo-

metry (Ptashnyk, in press) (Fig. 1b). This is justified as long as the distance between root hairs at the root surface, $2\pi a_r/n$, is comparable to the distance between the root hair tips, $2\pi(a_r + L_h)/n$, where a_r is the root radius, L_h is the root hair length and n is the number of root hairs in a root cross-section. In developing the following model we consider a periodic domain containing cylindrical root hairs orthogonal to a planar root surface. In this domain the distance between the root hairs, l, is the characteristic microscopic length scale; the root length scale, L, is the macroscopic length scale; the homogenization technique requires that $l \ll L$.

The importance of convection relative to diffusion can be estimated by the Péclet number (Roose & Kirk, 2009), $Pe = a_r u/D$ where u is the water flux and D is the diffusion coefficient. Typically, $a_r < 10^{-1}$ cm, $u = 10^{-7}$ cm s^{-1} and the diffusion coefficient, D, is $\leq 10^{-5}$ cm^2 s^{-1}, so $Pe \sim 10^{-3}$. This is true for both solution culture and soil. Thus, we can neglect convection. As a result, the nutrient concentration, c, is described by the diffusion equation:

$$\frac{\partial}{\partial t} c = \nabla \cdot (D \nabla c) \qquad \text{Eqn 1}$$

(where c is the nutrient concentration and D is the effective diffusion coefficient). In solution culture, $D = D_l$, where D_l is the diffusion coefficient in water, and, in soil, $D = D_l \theta f/(\theta + b)$, where θ is the volumetric water content, f is the diffusion impedance factor and b is the buffer power for sorption on soil surfaces. Initially, the nutrient concentration is assumed to be constant, in other words:

$$c = c_0 \quad \text{at } t = 0. \qquad \text{Eqn 2}$$

We chose the following boundary conditions:
(1) External boundaries – far away from the root and root hair zone, as well as at the upper and lower boundaries of the domain; we assume that there is no transfer of nutrients, such that:

$$-D \nabla c \cdot \boldsymbol{n} = 0. \qquad \text{Eqn 3}$$

This describes the case of an impermeable container.
(2) Root hair surface – nutrient uptake by root hairs is described by the uptake function, f_h, such that:

$$-D \nabla c \cdot \boldsymbol{n} = d \, f_h \qquad \text{Eqn 4}$$

(where $d = 1$ in the case of solution culture and $d = 1/(\theta + b)$ in the case of soil. In soil, the factor d describes that the root only takes up nutrients from the fluid phase).
(3) Root surface – nutrient uptake by the root is described by the uptake function, f_r, such that:

$$-D\nabla c \cdot \boldsymbol{n} = d\, f_{\mathrm{r}}. \qquad\qquad \text{Eqn 5}$$

In Eqns 3–5 the outer normals $\boldsymbol{n}$ are unit vectors that are orthogonal to the respective bounding surfaces and point outwards of the domain.

For uptake by root systems or individual roots under specified conditions of plant growth and nutrient supply, the relationship between influx and concentration at the root surface is usually given by a Michaelis–Menten-type relation (Tinker & Nye, 2000, and references therein). We know of no equivalent information for uptake by root hairs, but assume that a similar sort of relationship applies. Hence, we define:

$$f_{\mathrm{h}} = \frac{F_{\mathrm{h}}c}{K_{\mathrm{h}+c}} - E_{\mathrm{h}} \quad \text{and} \quad f_{\mathrm{r}} = \frac{F_{\mathrm{r}}c}{K_{\mathrm{r}+c}} - E_{\mathrm{r}} \qquad \text{Eqn 6}$$

(F, K and E are the maximal nutrient influx, the Michaelis constant and efflux, respectively; and subscripts h and r denote root hair and root, respectively). Alternative functional forms for f_{h} and f_{r} could also be used without any significant influence on the results presented here as long as the order of magnitudes of f_{h} and f_{r} do not change.

For most roots with root hairs, the ratio between the characteristic root hair scale, l, and root length scale, L, becomes small (i.e. $\epsilon = l/L \ll 1$). If the macroscopic length scale, L, is assumed to be 1 cm, ϵ lies between $6.1 \cdot 10^{-3}$ and $4.3 \cdot 10^{-2}$ for different plant species (see Table 2). We use the method of homogenization to analyse and simplify the model such that we do not explicitly consider every single root hair, but the cumulative effect of all root hair surfaces.

Homogenized model

In this section, we introduce three effective macroscopic models for nutrient transport and uptake near a root with root hairs. We derive them from the model that explicitly considers the root hair geometry given by Eqns 1–6. The full derivation (see Mathematical Notes S1) involves two steps. First, the single root hair scale model is nondimensionalized and, second, formal multiscale expansion is used to derive the effective equations valid on the root length scale. The method of nondimensionalization involves scaling the variables so that the new variables have no units (Fowler, 1997). In this form the model has fewer parameters and it is easier to analyze, in addition to revealing which processes dominate in any given parameter regime. For different limits of the root hair uptake rate we obtain the three different models. In the following, we present the effective equations in their dimensional forms.

In the homogenized model the domain V_{a} denotes the root hair zone and c_{a} denotes the averaged nutrient concen-

tration within this domain. The surrounding domain outside the root hair zone is denoted as V_{b} with the corresponding concentration c_{b}. The concentration c_{b} is given by:

$$\frac{\partial}{\partial t} c_{\mathrm{b}} = \nabla \cdot (D\nabla c_{\mathrm{b}}) \qquad\qquad \text{Eqn 7}$$

(where D is the effective diffusion coefficient; in water $D = D_{\mathrm{l}}$; and, in the case of soil, $D = D_{\mathrm{l}}\theta f\!/(\theta + b)$). On the boundary far away from the root and on the upper and lower boundaries of V_{b} we apply a no-flux boundary condition:

$$-D\nabla c_{\mathrm{b}} \cdot \boldsymbol{n} = 0 \qquad\qquad \text{Eqn 8}$$

(where $\boldsymbol{n}$ is the outer normal of the domain). This reflects the typical situation in a container, where nutrients cannot leave the domain.

Three different models can be derived for the root hair zone. The dimensionless parameter α is given by:

$$\alpha = \log_{\mathrm{e}}\left(\frac{dl}{DK_{\mathrm{h}}} F_{\mathrm{h}}\right) \Big/ \log_{\mathrm{e}}\left(\frac{l}{L}\right) \qquad \text{Eqn 9}$$

and distinguishes between those models (see Mathematical Notes S1, Eqn 16). The critical parameters determining α are both morphological and physiological parameters (i.e. the inter hair distance l; the factors $d = 1$ for solution culture and $d = 1/(\theta + b)$ for soil; root length L; the effective diffusion coefficient D; maximal nutrient influx into root hairs F_{h}; and the Michaelis–Menten constant for root hairs K_{h}). A review of parameter values from the literature for different plant species is presented in Table 2. If $\alpha \sim 1$, both uptake and diffusion are important processes; if $\alpha < 1$, uptake is negligibly small compared with diffusion; and if $\alpha > 1$, uptake is fast compared with diffusion.

Model 1 (case $\alpha \sim 1$) The most interesting situation arises when the rates of uptake and diffusion are comparable (i.e. $F_{\mathrm{h}}/K_{\mathrm{h}} \sim D/L$). This is the most common case in soil according to our literature search (see Table 2 and Eqn 9). In this case there is a dynamic development of a depletion zone within the root hair zone. This effectively takes into account the dynamic development of overlapping depletion zones between neighbouring root hairs. In this case the concentration inside the root hair zone, V_{a}, is described by an effective diffusion equation with the sink term describing the uptake by the root hairs:

$$\theta_{\mathrm{h}}\frac{\partial}{\partial t} c_{\mathrm{a}} - \nabla \cdot (\bar{D}\nabla c_{\mathrm{a}}) + d\frac{2\pi a_{\mathrm{h}}}{l^2} f_{\mathrm{a}} = 0 \qquad \text{Eqn 10}$$

(where θ_{h} is the volume fraction of the homogeneous medium in the root hair zone; $d = 1$ for solution culture or

Table 2 Morphological and physiological properties of roots and root hairs. The data were obtained from a literature survey for phosphate uptake by mildly phosphate starved plants

Plant	Root radius (a_r) 10^{-2} cm	Hair density (N)[1] cm^{-1}	Hair radius (a_h) 10^{-4} cm	Inter-hair distance $(l)^2$ 10^{-2} cm	Maximal influx (F_h) 10^{-7} μmol cm^{-2} s^{-1}	Michaelis constant (K_h) 10^{-3} μmol cm^{-3}	Efflux (E_h) 10^{-8} μmol cm^{-2} s^{-1}
Arabidopsis	0.6–0.65[d]	445[e]	3.2–3.3[f], 5.5[g], 8[h]	0.92–1.11	5.03, 7.66[j]	3.92, 6.37[j]	2.08[k]
Barley	0.75–0.85[c]	270–310[c]	–	1.23–1.41	15–29.7[i]	2.9–4.7[i]	0.58-0.71[i]
Bean[a]	1.45	490	5	1.36	2.76	0.4	6.9
Carrot[b]	1.07	1810	4	0.61	12.7	3.1	5.8
Lettuce[b]	1.24	1270	4.8	0.78	10.6	2	11.35
Onion	2.9[a], 2.25[b]	10[a], 1189[b]	5[a], 1[b]	4.27[a], 1.09[b]	2.68[a], 17[b]	0.4[a], 3.6[b]	6.7[a], 26[b]
Rape[a]	0.73	440	5	1.02	4.26	0.4	10.65
Ryegrass[a]	0.66	450	5	0.96	1.54	1.3	1.18
Russian Thistle[b]	0.56	890	3.9	0.63	3.9	2.7	3.42
Spinach[a]	1.07	710	5	0.97	4.10	0.4	10.25
Tomato	1[a], 1.07[b]	580[a], 1650[b]	5[a], 4.3[b]	1.04[a], 0.64[b]	9[a], 49.9[b]	0.4[a], 6.1[b]	22.5[a], 9.62[b]
Wheat	0.77[a], 1.08[b], 0.75–0.85[c]	460[a], 560[b], 240–380[c]	5[a], 5.7[b]	1.02[a], 1.1[b], 1.11–1.49[c]	2.21[a], 11.1[b]	2.3[a], 5.3[b]	0.96[a], 7.7[b]

[a]Föhse et al. (1991), [b]Itoh & Barber (1983), [c]Gahoonia et al. (1997), [d]Dolan et al. (1993), [e]Masucci & Schiefelbein (1994), [f]Bates & Lynch (2000a), [g]Galway et al. (1997), [h]Diet et al. (2004), [i]Nielsen & Schjørring (1983), [j]Narang et al. (2000), [k]Krannitz et al. (1991)
[1] Number of root hairs per cm root length.
[2] The calculated distance between the root hairs approximately the square root of the root surface area that is associated with a single root hair: $l = \sqrt{2a_r\pi/N}$.

$d = 1/(\theta + b)$ for soil; $2\pi a_h/l^2$ is the root hair surface area density; f_a is the root hair uptake described by a surface flux; and $\bar{D}$ is the effective diffusion matrix, in other words, it takes the diffusion impedance caused by the presence of root hairs into account). This is the dimensional form of Eqn 41 in the Mathematical Notes S1. The uptake f_a is given by:

$$f_a = \frac{L}{l}\left(\frac{F_h c_a}{K_h + c_a} - E_h\right) \qquad \text{Eqn 11}$$

which is the dimensional form of Eqn 46 in the Mathematical Notes S1.

Because of the impedance caused by the root hairs, the effective diffusion in the root hair zone is slower than that in the fluid or soil. The effective diffusion matrix $\bar{D}$ is given by:

$$\bar{D} = D\theta_h(D_{isotropic} + D_{corrector}) \qquad \text{Eqn 12}$$

(where $D_{isotropic}$ is the scaled diffusion matrix, and $D_{corrector}$ contains negative diagonal elements reducing the overall diffusion). The corrector is calculated in dependence on the root hair radius, a_h, and the inter hair distance, l; see Eqn 41 in the Mathematical Notes S1. If the root hairs are sparse, $a_h/l << 1$, the effective diffusion will be nearly identical to the diffusion coefficient D; whereas if the root hairs are dense, $0 << a_h/l < 0.5$, the effective diffusion $\bar{D}$ becomes small (see Fig. 1 in the Notes S1). Typical values for $a_h/l = 4.9 \cdot 10^{-2}$ are:

$$\frac{\bar{D}}{D(1 - \theta_{hair})} = \begin{pmatrix} 1 & 0 & 0 \\ 0 & 1 & 0 \\ 0 & 0 & 1 \end{pmatrix}$$
$$+ \begin{pmatrix} -7.5 \cdot 10^{-3} & 1.09 \cdot 10^{-8} & 0 \\ 1.09 \cdot 10^{-8} & -7.5 \cdot 10^{-3} & 0 \\ 0 & 0 & 0 \end{pmatrix} \qquad \text{Eqn 13}$$

(where D is the effective diffusion coefficient, and $\theta_{hair} = 0.01$ is the volume fraction of root hairs given by $a_h^2\pi/l^2$). In this specific example the corrector is based on the parameters for wheat plant (see Table 2) (Föhse et al., 1991).

The domain V_a is bounded at one side by the root surface. Nutrient flux into the root is described by:

$$-\bar{D}\nabla c_a \cdot \boldsymbol{n} = df_r \qquad \text{Eqn 14}$$

(where $\boldsymbol{n}$ is the outer normal to the root surface; $d = 1$ for solution culture or $d = 1/(\theta + b)$ for soil; and f_r describes the flux into the root (see Eqn 5). The other boundary is between the root hair zone, V_a, and the domain V_b, where continuity of concentration and continuous flux boundary conditions are applied:

$$c_a = c_b, \bar{D}\nabla c_a \cdot \boldsymbol{n} = D\nabla c_b \cdot \boldsymbol{n} \qquad \text{Eqn 15}$$

(where $\boldsymbol{n}$ is the outer normal of the root hair domain, V_a, pointing into the domain V_b).

In the Mathematical Notes S1 we derived the effective equations using multiscale expansion. A proof that these equations are actually the unique limit of this homogenization problem when $\epsilon \to 0$ can be found in Ptashnyk (in press).

Model 1 describes the root hair uptake with a sink term and in this sense it is similar to the model proposed by Bhat *et al.* (1976) and Geelhoed *et al.* (1997). However, the main difference is that the diffusion impedance caused by the presence of root hairs is also explicitly taken into account in our model.

Model 2 (case α > 1) When $\alpha > 1$, nutrient uptake into the root hairs is vanishingly small. The average concentration, c_a, is described by:

$$\theta_h \frac{\partial}{\partial t} c_a - \nabla \cdot (\bar{D} \nabla c_a) = 0. \qquad \text{Eqn 16}$$

The only difference to Model 1 is that Eqn 10 is replaced with Eqn 16.

This describes the situation where there is no significant active nutrient uptake within the root hair zone. The concentration gradient is solely created by the flux into the root. The root hairs are impeding the nutrient flux, but they are not influencing the concentration profile. There is no corresponding model in the literature describing this possibility, although a scenario similar to this has been discussed previously by Roose (2000). Our parameter estimation in the section 'Parameter values' suggests that this model does not apply for most plant species. However, it can apply in strongly sorbing soils, particularly for root-hair-defective mutants (e.g. of *Arabidopsis*). Equation 9 enables us to exactly determine parameter regimes where it is possible to neglect root hair uptake.

Model 3 (case α < 1) When $\alpha < 1$, the nutrient uptake by the root hairs is very large. Thus, nutrient concentration profiles between neighbouring root hairs start overlapping rapidly. This is the most common case in solution culture according to our literature search (see Table 2 and Eqn 9). The average concentration reaches its equilibrium almost instantaneously and thus the dynamic development of a concentration gradient in the root hair zone can be neglected. The concentration, c_a, within the root hair zone is constant and given by the solution to $f_h = 0$. For the case of Michaelis–Menten kinetics, it is given by Eqn 6:

$$\frac{F_h c_a}{K_h + c_a} - E_h = 0. \qquad \text{Eqn 17}$$

It follows that:

$$c_a = \frac{E_h K_h}{F_h - E_h} \qquad \text{Eqn 18}$$

in the root hair zone, V_a.

The boundary of the domain, V_b, to the root hair zone, V_a, is described with a Dirichlet boundary condition:

$$c_b = c_a. \qquad \text{Eqn 19}$$

In this model, root hairs effectively extend the root radius by the root hair length, and thus Model 3 corresponds to the model proposed by Passioura (1963).

Parameter values

We obtained morphological and physiological parameters for phosphate uptake by roots and root hairs from a survey of the literature. The parameters for different plant species are given in Table 2. For a particular plant species, maximum rates of influx into roots and the concentration-dependence of influx (as summarized in the Michaelis–Menten parameters in Eqn 6) vary with the plant's internal nutritional status, growth stage and other conditions (Marschner, 1995; Tinker & Nye, 2000). Hence, in a plant that has been starved of phosphate before measurements of influx are made, root transport systems will be up-regulated compared with phosphate-sufficient plants, and influx will be correspondingly greater. A complete description of the uptake properties of roots of a particular species is therefore complicated and beyond the scope of the current model. Hence, an experiment to paramaterize our model might use plants in nutrient solution under moderate phosphate stress before measurement of short-term influx at different concentrations of phosphate (Narang *et al.*, 2000; Nielsen & Schjørring, 1983). Other methods include using radio-labelled phosphorous in soil for measuring short-term kinetics, uptake measurements between two harvests (Föhse *et al.*, 1991) and the depletion method of Claassen & Barber (1974) (Itoh & Barber, 1983; Krannitz *et al.*, 1991). Values of F_h, K_h and E_h are given in Table 2 for phosphate uptake by different plant species.

The parameter E_h in Eqn 6 is calculated from influx at the minimum concentration at which roots can maintain a net influx of phosphate, C_{min}, according to:

$$E_h = \frac{F_h C_{min}}{(K_h + C_{min})} \qquad \text{Eqn 20}$$

(where C_{min} is typically in the range of 0.01–0.12 μM for different plant species (Tinker & Nye, 2000)).

The initial concentration of phosphate is taken to be $5 \cdot 10^{-4}$ $\mu mol\ cm^{-3}$. This is typical for a soil in which phosphate is likely to be limiting (Föhse *et al.*, 1991; Tinker

& Nye, 2000). As soil-specific parameters we chose volumetric water content $\theta = 0.3$, impedance factor $f = 0.3$, and soil buffer power $b = 239$. These are typical values often found in soils (Tinker & Nye, 2000; Barber, 1995; Roose *et al.*, 2001) and will therefore be used in our simulations.

From the parameter values in Table 2 we found that the dimensionless parameter α is between 0 and 1. Thus, we present simulation results for Models 1 and 3. We implemented the effective models given above using the finite element analysis package Comsol Multiphysics 3.5 (http://www.comsol.com/).

Results

In the following sections we illustrate the application of the three models by considering the effects of root hair properties on phosphate depletion in solution culture and soil. Changes in concentration only occur with distance from and along the root axis. Therefore, it is sufficient to consider axial symmetry.

In the first example we compare Models 1 and 3 with parameters relating to wheat and tomato. We show the one-dimensional concentration profiles of phosphate with respect to the distance from the root axis. The position along the root axis is at the centre of the root hair zone; the root hairs are 0.033 cm long.

In Model 1 (case $\alpha \sim 1$), root hairs take up phosphate according to the model described in Eqns 7, 8 and 10–15. In Model 3 (case $\alpha < 1$), the uptake of phosphate by root hairs is very fast, leading to effectively instantaneous uptake in comparison with diffusion through the solution. Thus, the root radius is essentially extended by the root hair length, and gradients within the root hair zone can be neglected. The model describing this situation is given in Eqns 7, 8, 18 and 19. In Fig. 2 we show the gradient caused by depletion, for solution culture and soil. After 1 d the depletion zone in solution culture extends up to 3 cm away from the root surface (Fig. 2a). In comparison, this zone is only 0.12 cm wide in soil (Fig. 2b). The dynamic development of the gradient can be seen in the close-up of the root hair zone. In solution culture, the depletion in the root hair zone is in the order of seconds (Fig. 2c), whereas, in soil, it is in the order of hours (Fig. 2d).

In the second example we analyse the effect of root growth on phosphate depletion and uptake in Model 1. The root hair zone is situated 0.5 cm behind the root tip and is 1 cm in length along the root; the root hairs are 0.033 cm long. The root tip is assumed to grow at a rate of 2 cm d^{-1} (Watt *et al.*, 2006). Changes with respect to the root surface and along the root axis are considered. Fig. 3 shows the depletion zones around a root after 2 d, for both solution culture and soil, according to three different scenarios. In scenario 1 it is assumed that both root and root hairs are taking up phosphate. In scenario 2 root uptake is neglected, and in scenario 3 only root uptake is considered. In this way we show the effect of the root hair zone on the depletion of phosphate. In the case of solution culture (Fig. 3a), the root hairs cause a strong depletion in scenarios 1 and 2, while the depletion caused by the root only in scenario 3 is negligible because of fast replenishment in the absence of sorption. In soil, as a result of strong sorption, the width of the depletion zone is maintained at the width of the root hair zone even after the root hair zone, has grown further downwards (Fig. 3b). The root on its own causes a typical depletion profile, which is steeper, but more narrow, than in solution culture. We present the dynamic development of the depletion zones in the three scenarios in Supporting Information Videos S1–S6.

The corresponding cumulative phosphate uptake is shown in Fig. 4. After 2 d, the overall uptake in solution culture in the two scenarios where root hairs are absorbing phosphate is larger than in the scenario where only the root is absorbing. The uptake is 2.7 and 1.7 times larger for scenarios 1 and 2, respectively. The contributions of root and root hairs to overall uptake in scenario 1 is represented by the dashed lines in Fig. 4a. After 2 d, roots contributed to 36% of the overall uptake and root hairs contributed to 64% of the overall uptake. This situation is different in soil. When root hairs are taking up phosphate the depletion is so strong that the root uptake becomes negligibly small. Therefore, total phosphate uptake of scenarios 1 and 2 are similiar (Fig. 4b). Root uptake is only significant when no earlier depletion, by root hairs, occurs. Root and root hair uptake is 28 times larger than root uptake alone. The root hair zone contributes 96% to the overall uptake and the root contributes 4% to the overall uptake.

Discussion

We presented a root hair scale model for nutrient uptake by root hairs and derived three different effective models, which were dependent on the morphological and physiological properties of root hairs. The first model describes the effect of root hairs with a sink term in the diffusion equation. This results in the development of a concentration gradient within the root hair zone. The second model describes a situation where root hair uptake is negligibly small. In the third model all the nutrients inside the root hair zone are taken up instantaneously, and thus the root hairs effectively increase the root radius by the root hair length. Based on our model analysis using published morphological and physiological parameters we have shown that Model 1 (case $\alpha \sim 1$) and Model 3 (case $\alpha < 1$) are primarily applicable in real systems. Model 2 is suitable for strongly sorbing soils, particularly for root hair-defective mutants. Whether we are in a solution culture or homogeneous soil system
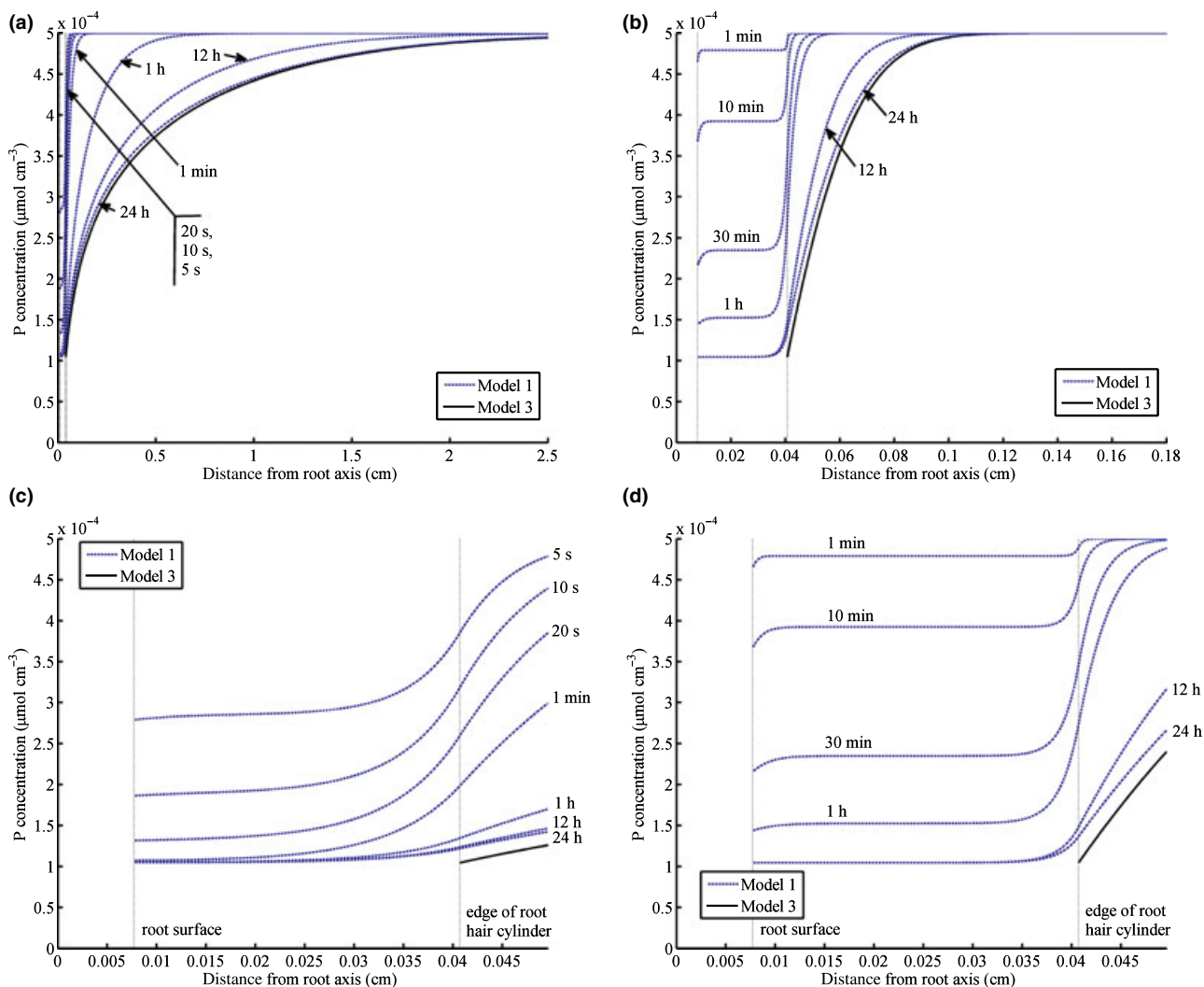
Fig. 2 The effect of uptake, by root hairs, on phosphate concentration-distance profiles of phosphate near the root axis in (a) solution culture and (b) soil. The graphs shown in (c) and (d) are magnifications of the root hair zones in graphs (a) and (b), respectively. The parameter values are the same as those given in Table 2 for wheat. Depletion zones predicted by Models 1 and 3 agree for $t \geq 24$ h.

only changes the characteristic timescale but not the models.

In Model 1, a sink term for root hair uptake in the conservation equation results in phosphate depletion in the root hair zone. Such sink terms have been developed before for soil systems (de Willigen & van Noordwijk, 1994; Geelhoed *et al.*, 1997; Bhat *et al.*, 1976; Baldwin *et al.*, 1973); in the following we discuss the differences between our model and those sink terms. First previous work derived a macroscopic equation using a sink term for root hair uptake, which is based on a concentration averaged around the root hairs. We essentially follow this approach but derive the sink term in a mathematically rigorous way using the method of homogenization. Furthermore, we can predict, from root morphological and physiological parameters, when this specific form of sink term is valid. Further still, in

all previous models the impedance of diffusion caused by the root hairs has been neglected. Previous models consider impedance to be caused by soil particles but not by root hairs. Finally, the sink terms are based on steady-state approximations of linear (Bhat *et al.*, 1976; Baldwin *et al.*, 1973) or zero sink (Geelhoed *et al.*, 1997; de Willigen & van Noordwijk, 1994) boundary conditions at the root hair surface. In contrast to previous models, our model uses nonlinear Michaelis–Menten boundary conditions. In Model 3, root hairs effectively extend the root radius, and phosphate inside the root hair zone is taken up instantaneously. Such an 'equivalent cylinder' has already been discussed by Passioura (1963). We have been able to determine parameter regimes where each model is valid. When the characteristic velocity scale of uptake is in the same order as that of diffusion, $F_h/K_h : D/L \sim 1$, Model 1
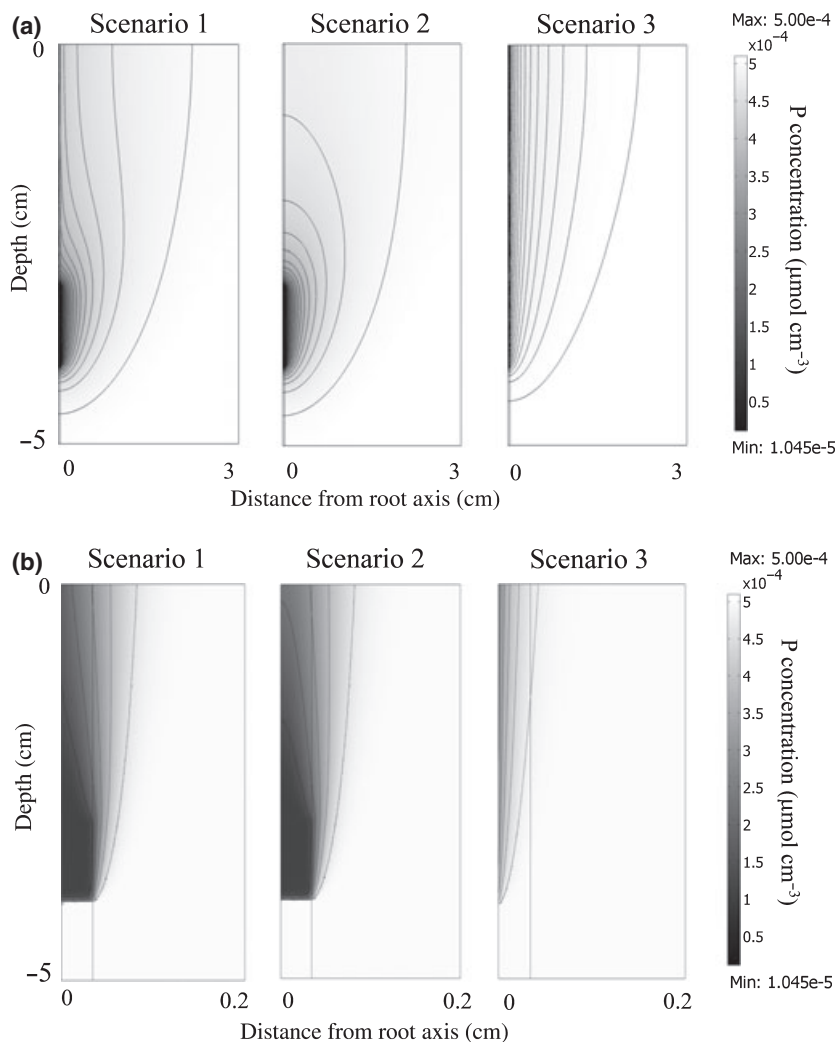
(a)

(b)

Fig. 3 Depletion profiles around a growing root after 2 d, calculated using Model 1. The parameter values are the same as those given in Table 2 for wheat with a root elongation rate = 2 cm d^{-1}. In scenario 1, both root and root hairs take up phosphate (individual contributions are shown in Fig. 4). In scenario 2, only the root hairs take up phosphate. In scenario 3, only the root takes up phosphate.

applies. When $F_h/K_h : D/L \sim \epsilon^{-1}$, Model 3 is suitable. For typical values $D = 10^{-5}$ cm^2 s^{-1}, $l = 0.01$ cm, and $L = 1$ cm, the characteristic velocity scale of uptake needs to be in the order of 10^{-5} cm s^{-1} for Model 1 and larger than 10^{-3} cm s^{-1} for Model 3.

The models presented here provide an explanation of phosphate uptake by various plants with different root hair architectures. Previous studies have demonstrated that root hairs are important in phosphate uptake and that the root hair length is influenced by the external phosphate concentration (Bates & Lynch, 1996). The fact that the width of the phosphate-depletion zones around nonmycorrhizal roots are closely related to root hair length (Marschner, 1995) is demonstrated in Fig. 3. This provides a mechanism for the plant to maximize phosphate uptake under limiting conditions.

The validity of our model could be tested by measuring phosphate-uptake dynamics in root hair mutants. Root hair mutants are available in *Arabidopsis* (Schiefelbein & Somerville, 1990; Grierson *et al.*, 2001), rice

(Ma *et al.*, 2001), barley (Gahoonia *et al.*, 2001), tomato (Hochmuth *et al.*, 1985) and *Zea mays* (Wen & Schnable, 1994). The *Arabidopsis rhd2* and *rhd6* mutants have altered hair initiation and elongation, respectively, and both have reduced shoot biomass compared with the wild type when grown under phosphate-limiting conditions (Bates & Lynch, 2000b). This was interpreted as reflecting a reduced ability by the *rhd2* and *rhd6* mutants to take up phosphate, or may reflect an inability to respond to phosphate-limiting conditions. Our model can be utilized to explain alterations in phosphate uptake by these mutants. In particular, we can predict how quickly the concentrations in the root hair zone will drop to zero. This indicates the timescale of measurements required to observe the dynamics of the depletion zone development. The parameter α ranges between 0.37 and 0.54 for the morphological and physiological parameters of *Arabidopsis* given in Table 2. Thus, they are at the border between Model 1 (case $\alpha \sim 1$) and Model 3 (case $\alpha < 1$). This means that the root hairs deplete the root hair zone very
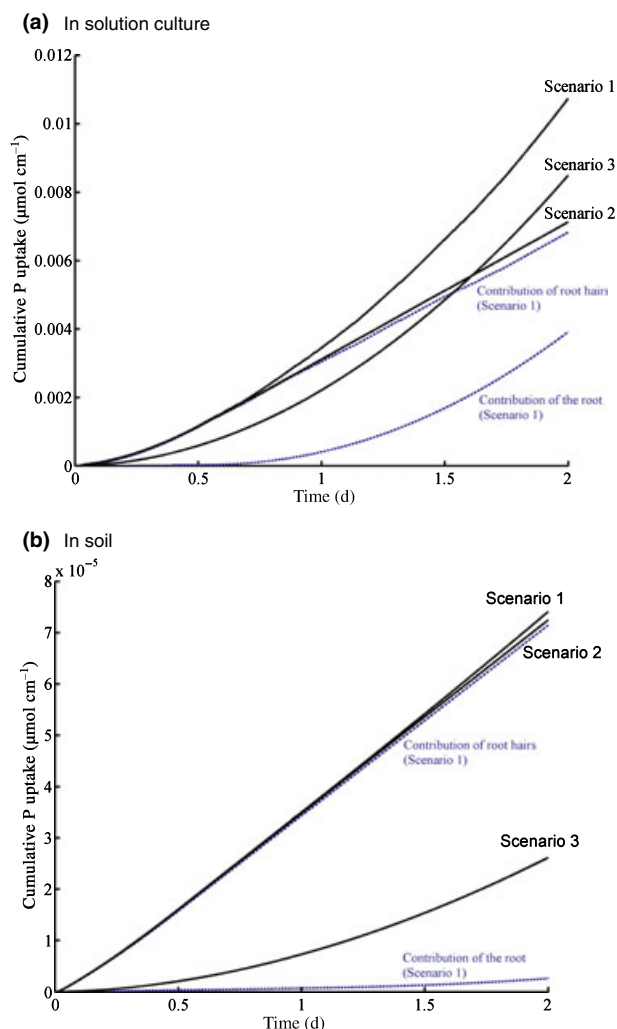
(a) In solution culture

(b) In soil

Fig. 4 Cumulative phosphate uptake by a growing root over 2 d, calculated using Model 1. The parameter values are the same as those given in Table 2 for wheat with a root elongation rate = 2 cm d^{-1}. Solid lines show overall uptake in scenarios 1 to 3. Dashed lines show the contributions of root and root hairs to the overall uptake in scenario 1.

quickly, but Model 3 might still overestimate uptake. We suggest using the most inclusive model in this case, in other words, Model 1, which includes the sink term for phosphate uptake in the root hair zone. In this case, the timescale of depletion is given by

$$[t] = \frac{\theta + b}{2\pi a_h} \frac{K_h}{F_h} \frac{l^3}{L}.$$

For the *Arabidopsis* species given in Table 2, the timescale of depletion ranges from 0.79 to 8.61 s in solution culture and from 3.16 to 34.36 min in soil. In a hydrogel with the same impedance factor as soil, the development of the depletion profile would be slowed down in comparison to nutrient solution culture and thus be more readily observa-

ble. If the morphological and physiological parameters for *rhd6* and *rhd2* are known, our model can predict the α-regime and timescale of depletion compared with wild-type species. This can help to optimize the design of a specific validation experiment.

Acknowledgements

References

Baldwin JP, Nye PH, Tinker PB. 1973. Uptake of solutes by multiple root systems from soil – III – A model for calculating the solute uptake by a randomly dispersed root system developing in a finite volume of soil. *Plant and Soil* **38**: 621–635.

Barber SA. 1995. *Soil nutrient bioavailability: a mechanistic approach*. New York, NY, USA: John Wiley & Sons, Inc.

Bates TR, Lynch JP. 1996. Stimulation of root hair elongation in *Arabidopsis thaliana* by low phosphorus availability. *Plant, Cell & Environment* **19**: 529–538.

Bates TR, Lynch JP. 2000a. The effciency of *Arabidopsis thaliana* (Brassicaceae) root hairs in phosphorus acquisition. *American Journal of Botany* **87**: 964–970.

Bates TR, Lynch JP. 2000b. Plant growth and phosphorus accumulation of wild type and two root hair mutants of *Arabidopsis thaliana* (Brassicaceae). *American Journal of Botany* **87**: 958–963.

Bhat KKS, Nye PH, Baldwin JP. 1976. Diffusion of phosphate to plant roots in soil – IV. The concentration distance profile in the rhizosphere of roots with root hairs in a low-P soil. *Plant and Soil* **44**: 63–72.

Claassen N, Barber SA. 1974. A method for characterizing the relation between nutrient concentration and flux into roots of intact plants. *Plant Physiology* **54**: 564–568.

de Willigen P, van Noordwijk M. 1994. Mass flow and diffusion of nutrients to a root with constant or zero-sink uptake I. Constant uptake. *Soil Science* **157**: 162–170.

Diet A, Brunner S, Ringli C. 2004. The *enl* mutants enhance the *lrx1* root hair mutant phenotype of *Arabidopsis thaliana*. *Plant and Cell Physiology* **45**: 734–741.

Dolan L, Janmaat K, Willemsen V, Linstead P, Poethig S, Roberts K, Scheres B. 1993. Cellular organisation of the *Arabidopsis thaliana* root. *Development* **119**: 71–84.

Föhse D, Claassen N, Jungk A. 1991. Phosphorus efficiency by plants. *Plant and Soil* **132**: 261–272.

Fowler A. 1997. *Mathematical models in the applied sciences*. Cambridge, UK: Cambridge University Press.

Gahoonia TS, Care D, Nielsen NE. 1997. Root hairs and phosphorus acquisition of wheat and barley cultivars. *Plant and Soil* **191**: 181–188.

Gahoonia TS, Nielsen NE, Joshi, PA, Jahoor A. 2001. A root hairless barley mutant for elucidating genetic of root hairs and phosphorus uptake. *Plant and Soil* **235**: 211–219.

Galway ME, Heckman Jr JW, Schiefelbein JW. 1997. Growth and ultrastructure of *Arabidopsis* root hairs: the *rhd3* mutation alters vacuole enlargement and tip growth. *Planta* **201**: 209–218.

Geelhoed JS, Mous SLJ, Findenegg GR. 1997. Modeling zero sink nutrient uptake by roots with root hairs from soil: comparison of two models. *Soil Science* **162**: 544–553.

Grierson CS, Parker JS, Kemp AC. 2001. *Arabidopsis* genes with roles in root hair development. *Journal of Plant Nutrition and Soil Science* **164**: 131–140.

Hochmuth GJ, Gabelmann WH, Gerloff GC. 1985. A gene affecting tomato root morphology. *HortScience* **20**: 1099–1101.

Hornung U. 1997. *Homogenization and porous media.* New York, NY, USA: Springer.

Itoh S, Barber SA. 1983. Phosphorus uptake by six plant species as related to root hairs. *American Society of Agronomy* **75**: 457–461.

Krannitz PG, Aarssen LW, Lefebvre DD. 1991. Shot-term competition for phosphate between two genotypes of *Arabidopsis thaliana* (L) Heynh. *New Phytologist* **119**: 389–396.

Ma JF, Goto S, Tamai K, Ichii M. 2001. Role of root hairs and lateral roots in silicon uptake by rice. *Plant Physiology* **127**: 1773–1780.

Marschner H. 1995. *Mineral nutrition of higher plants.* London, UK: Academic Press.

Masucci JD, Schiefelbein JW. 1994. The *rhd6* mutation of *Arabidopsis thaliana* alters root-hair initiation through an auxin- and ethylene-associated process. *Plant Physiology* **106**: 1335–1346.

Narang RA, Bruene A, Altmann T. 2000. Analysis of phosphate acquisition efficiency in different *Arabidopsis* accessions. *Plant Physiology* **124**: 1786–1799.

Nielsen NE, Schjørring JK. 1983. Efficiency and kinetics of phosphorus uptake from soil by various barley genotypes. *Plant and Soil* **72**: 225–230.

Passioura JB. 1963. A mathematical model for the uptake of ions from the soil solution. *Plant and Soil* **18**: 225–238.

Pavliotis G, Stuart A. 2008. *Multiscale methods averaging and homogenization.* New York, NY, USA: Springer.

Ptashnyk M. (in press). Derivation of a macroscopic model for nutrient uptake by hairy-roots. *Nonlinear Analysis: Real World Applications* doi: 10.1016/j.nonrwa.2008.10.063.

Roose T. 2000. *Mathematical model of plant nutrient uptake.* Ph.D. thesis, University of Oxford, Oxford, UK.

Roose T, Fowler AC, Darrah PR. 2001. A mathematical model of plant nutrient uptake. *Journal of Mathematical Biology* **42**: 347–360.

Roose T, Kirk GJD. 2009. The solution of convection-diffusion equations for solute transport to plant roots. *Plant and Soil* **316**: 257–264.

Schiefelbein JW, Somerville C. 1990. Genetic control of root hair development in *Arabidopsis thaliana. Plant Cell* **2**: 235–243.

Tinker PB, Nye PH. 2000. *Solute movement in the rhizosphere.* Oxford, UK: Oxford University Press.

Watt M, Sil WK, Passioura JB. 2006. Rates of root and organism growth soil conditions and temporal and spatial development of the Rhizosphere. *Annals of Botany* **97**: 839–855.

Wen TJ, Schnable PS. 1994. Analysis of mutants of three genes that influence root hair development in *Zea mays* (Gramineae) suggest that root hairs are dispensable. *American Journal of Botany* **81**: 833–842.

Wissuwa M. 2003. How do plants achieve tolerance to phosphorus deficiency? Small causes with big effects. *Plant Physiology* **133**: 1947–1958.

Zhang Y, Lynch JP, Brown KM. 2003. Ethylene and phosphorus availability have interacting yet distinct effects on root hair development. *Journal of Experimental Botany* **54**: 2351–2361.

Supporting Information

Additional supporting information may be found in the online version of this article.

Notes S1. Derivation of the model.

Video S1. Animation showing the dynamic development of the depletion zone in solution culture for Scenario 1 (corresponding to Fig. 3a).

Video S2. Animation showing the dynamic development of the depletion zone in solution culture for Scenario 2 (corresponding to Fig. 3a).

Video S3. Animation showing the dynamic development of the depletion zone in solution culture for Scenario 3 (corresponding to Fig. 3a).

Video S4. Animation showing the dynamic development of the depletion zone in soil for Scenario 1 (corresponding to Fig. 3b).

Video S5. Animation showing the dynamic development of the depletion zone in soil for Scenario 2 (corresponding to Fig. 3b).

Video S6. Animation showing the dynamic development of the depletion zone in soil for Scenario 3 (corresponding to Fig. 3b).